

# EXAMINING THE EFFECTS OF OXYGEN DOPING ON SRF CAVITY PERFORMANCE\*

H. Hu<sup>†</sup>, Y.-K. Kim, University of Chicago, Chicago, IL, USA  
D. Bafia, Fermi National Accelerator Laboratory, Batavia, IL, USA

## Abstract

Superconducting radiofrequency (SRF) cavities are resonators with extremely low surface resistance that enable accelerating cavities to have extremely high quality factors ( $Q_0$ ). High ( $Q_0$ ) decreases the capital required to keep accelerators cold by reducing power loss. The performance of SRF cavities is largely governed by the surface composition of the first 100 nm of the cavity surface. Impurities such as oxygen and nitrogen have been observed to yield high  $Q_0$ , but their precise roles are still being studied. Here, we compare the performance of cavities doped with nitrogen and oxygen in terms of fundamental material properties to understand how these impurities affect performance. This enables us to have further insight into the underlying mechanisms that enable these surface treatments to yield high  $Q_0$  performance.

## INTRODUCTION

The role of impurities in the RF layer, the first 100 nm of the cavity surface, is critical in superconducting radiofrequency (SRF) cavity performance. Nitrogen doping is a surface treatment which introduces a dilute concentration of nitrogen impurities uniformly into the RF layer [1]. Nitrogen doped cavities have displayed quality factors ( $Q_0$ ) of  $> 4 \times 10^{10}$  and maximum accelerating gradients ( $E_{acc}$ ) of  $> 38$  MV/m [1]. Low temperature baking (LTB) is a surface treatment which relies on the diffusion of oxygen from the native oxide to mitigate high field Q-slope (HFQS) and improve  $Q_0$  at high  $E_{acc}$  [2]. Motivated by these studies on LTB, we conduct initial studies on a new surface treatment called oxygen doping. Oxygen doping introduces oxygen impurities uniformly into the RF layer to achieve doping-like performance without any extrinsic impurities [3]. Oxygen doping has been shown to display high  $Q_0$  of  $4.2 \times 10^{10}$  at 20 MV/m with a maximum  $E_{acc}$  of 34 MV/m [4]. In addition, oxygen doped cavities display phenomena in performance that are characteristic of a nitrogen doped cavity: the anti-Q slope in which BCS resistance decreases with field, and a dip in resonant frequency near the transition temperature ( $T_c$ ). This work is an extension of the initial comparisons of oxygen doping and nitrogen doping presented in Ref. [4] by comparing the fundamental material properties of transition temperature, superconducting gap and mean free path.

\* Work supported by the Fermi National Accelerator Laboratory, managed and operated by Fermi Research Alliance, LLC under Contract No. DE-AC02-07CH11359 with the U.S. Department of Energy; the University of Chicago.

<sup>†</sup> hannahhu@uchicago.edu

## EXPERIMENTAL METHOD

RF tests were conducted on a single-cell TESLA shaped Nb cavity of resonant frequency 1.3 GHz. The cavity was baselined with an 800°C degassing treatment and 40 μm electropolishing (EP) removal [3]. The cavity was then treated according to the following steps: (1) *in-situ* bake at 200°C in an UHV furnace while maintaining  $10^{-6}$  Torr, (2) HF rinse, (3) second round of HF rinse.

After each step of treatment, the cavity was evacuated and assembled at the vertical test stand (VTS) with two flux gates at the equator, resistance temperature detectors (RTDs), and a Helmholtz coil. The cavity was cooled down to 4.2 K with the fast cool down protocol to minimize the trapping of magnetic flux before it was further pumped down to be tested at first 2 K and then  $< 1.5$  K (lowT) [3]. At each temperature, the  $Q_0$  vs.  $E_{acc}$  performance is recorded in continuous wave (CW) operation. Next, the liquid helium is boiled off using heaters to gradually warm the cavity up past transition temperature ( $T_c$ ) at a rate of  $< 0.1$  K/min [5]. The change in resonant frequency ( $f_0$ ) in temperature is recorded with a vector network analyzer.

Additionally, cavity cutouts of 1 cm in diameter were treated with a similar oxygen doping treatment of a 205°C bake for 19 hours. The sample was analyzed with time of flight secondary ion mass spectrometry (TOF-SIMS) to determine the concentration of each impurity present in the sample at each depth.

## RESULTS AND DISCUSSION

The performance and material properties for each of three treatment steps is compared to that of a nitrogen doped single-cell cavity with a treatment recipe of 2/0 + 5 μm EP. The data for the nitrogen doped cavity is reproduced from Ref. [6].

There are two key features in N doped cavity performance that are also displayed in O doped cavities. Shown in Fig. 1 is the behavior of  $Q_0$  vs  $E_{acc}$  at 2 K. During the test labeled O doped, the cavity experienced an initial quench at around 19 MV/m from field emissions. This trapped magnetic flux and decreased  $Q_0$ . The test after HF rinse 2 experienced a quench due to multipacting at 20 MV/m, which prevented data from being taken until 25 MV/m and also trapped flux. All three tests display the anti-Q slope phenomenon where  $Q_0$  increases with  $E_{acc}$ . Anti-Q slope in N doped cavities arises from a decrease in the BCS surface resistance with field, and this was shown to also be the case for O doped cavities [4, 7].

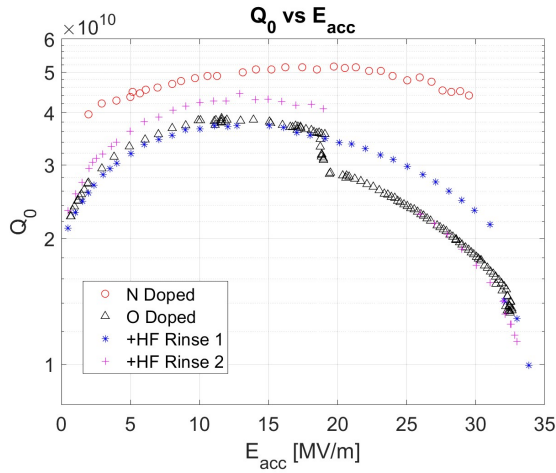


Figure 1:  $Q_0$  vs.  $E_{acc}$  data taken at 2 K acquired at Fermilab's VTS system. Plot reproduced from [4].

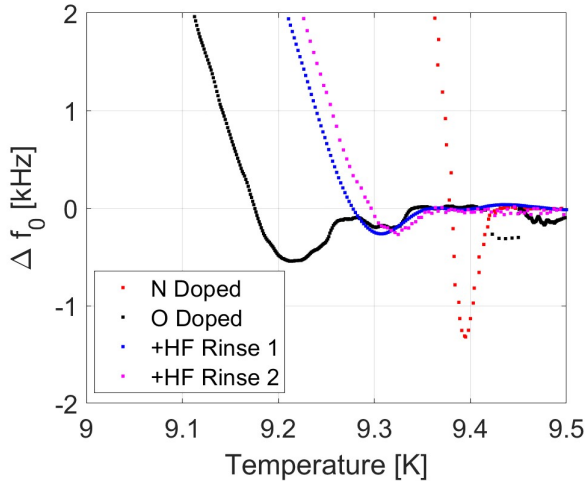


Figure 2: Frequency response with temperature showing anomalous resonant frequency variation.

The other feature is an anomalous decrease in  $f_0$  just before  $T_c$ , displayed in Fig. 2. The frequency data has been corrected to account for any variations in pressure in the dewar. Two types of dip behavior are observed. The two curves after HF rinse exhibit only a dip before  $T_c$ ; this dip is characteristic of a N doped cavity and the magnitude is directly related to the degree of the anti-Q slope [5]. The curve from the O doped cavity displays a “dip+bump” characteristic behavior that has been observed in a N infused cavity [5]. HF rinsing also halves the magnitude of the dip from 0.54 to 0.25. Additionally, all three steps of the O doped and HF rinsed treated cavity experience a similar degree of  $T_c$  suppression. This  $T_c$  suppression and the weakening of superconductivity may be a source of the high field losses observed in Ref. [4]. The experimental  $T_c$  and magnitude of frequency dip ( $\Delta f_{dip}$ ) are displayed in Table 1.

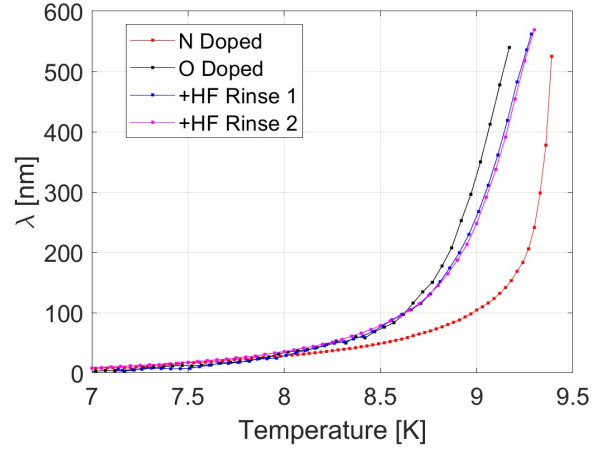


Figure 3: Change in penetration depth with temperature.

Each  $f(T)$  curve was converted to  $\lambda(T)$ , shown in Fig. 3, using Slater's theorem:

$$\Delta\lambda(T) = \frac{-G\Delta f_0(T)}{\mu_0\pi f_0^2(T_0)} \quad (1)$$

where  $G = 270 \Omega$ ,  $\mu_0 = 1.26 \times 10^{-6}$  H/m, and  $f_0(T_0)$  which is the frequency at which below temperature  $T_0$ ,  $f_0$  is no longer temperature dependent [8]. This curve is fitted based on Halbritter's SRIMP routine to obtain the parameters of superconducting gap ( $\Delta$ ) and average of the effective mean free path (mfp) over the first 200 nm [9]. The fitted  $\Delta$  and mfp for each treatment is presented in Table 1. The fixed parameters for the fit are the penetration depth at 0 K ( $\lambda_L$ ) of 39 nm and the coherence length ( $\xi_0$ ) of 62 nm. The superconducting gap,  $\Delta$ , for the oxygen doped cavity has an average of  $1.95 \pm 0.20$  meV, comparable to  $2.10 \pm 0.08$  meV for nitrogen doped. This suggests that the oxygen doping treatment is effective at reducing BCS surface resistance and quasi-particle introduced losses.

The average mfp over the first 200 nm of the surface following an oxygen doping treatment of 200°C for 20 hours is of an order of magnitude smaller than that of nitrogen doping. The oxygen doped mfp values are consistent with what Ciovati *et al.* measured in a study of LTB baking temperature [10]. In addition, the agreement in mfp for these three tests suggests that HF rinsing does not have a significant effect on the surface impurity profile. This was further confirmed by examining the SIMS data (shown in Fig. 4) of  $O^-$  impurities in an oxygen doped (205°C × 19 hours [11]) surface compared to  $NbN^-$  impurities in a nitrogen doped (2/0 + 5 μm EP [6]) surface. Although the impurities do not extend as far into the bulk for O doping as with N doping, within the rf layer, the concentration of  $O^-$  is approximately uniform. The removal of  $\approx 9$  nm of material through 2 rounds of HF rinsing is not on a scale large enough to change the overall concentration of impurities [12].

Table 1: Summary of Material Properties and SRIMP Fit Parameters

	$\Delta$ [meV]	mfp [nm]	$T_c$ [K]	$\Delta f_{\text{dip}}$ [kHz]
N Doped	$2.10 \pm 0.08$ [6]	$125.1 \pm 37.8$ [6]	9.42	1.31
O Doped	$2.18 \pm 0.04$	$17.99 \pm 1.12$	9.34	0.54
+ HF Rinse 1	$1.69 \pm 0.02$	$14.52 \pm 0.56$	9.36	0.26
+ HF Rinse 2	$1.98 \pm 0.03$	$16.79 \pm 0.79$	9.36	0.25

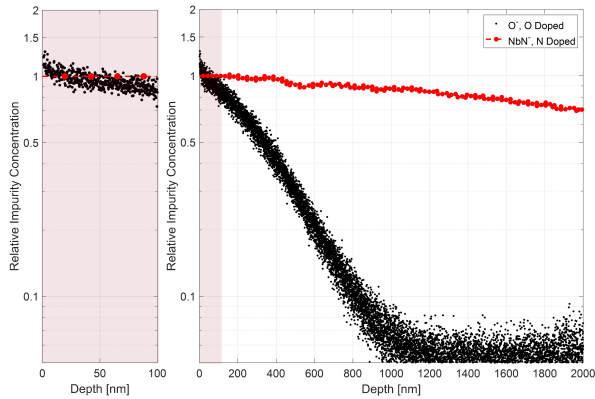


Figure 4: (Right) SIMS impurity profiles of  $O^-$  in an oxygen doped sample and  $NbN^-$  in a nitrogen doped sample normalized to the surface concentration. (Left) Zoomed in plot showing the uniform concentration of impurities in the rf surface.

## CONCLUSION

The phenomena of anti-Q slope, and anomalous frequency dip as well as similarities in surface impurity profiles between N doping and O doping have confirmed the viability of O doping as a treatment capable of achieving high  $Q_0$ . Studying fundamental material properties of  $T_c$ , mfp and  $\Delta$ , gives additional methods of comparing these two treatments. Further SIMS studies, including the use of standards to determine absolute concentration of impurities in a sample, are needed to reconcile the order of magnitude difference in mfp.

## REFERENCES

[1] A. Grassellino *et al.*, “Nitrogen and argon doping of niobium for superconducting radio frequency cavities: a pathway to highly efficient accelerating structures”, *Supercond. Sci. Tech.*, vol. 26, pp. 102001, 2013. doi: 10.1088/0953-2048/26/10/102001

[2] A. Romanenko *et al.*, “Proximity Breakdown of Hydrides in Superconducting Niobium Cavities”, *Supercond. Sci. Tech.*, vol. 26, pp. 035003, 2013. doi: 10.1088/0953-2048/26/3/035003

[3] D. Bafia *et al.*, “The role of oxygen concentration in niobium SRF cavities”, in *Proc. SRF’21*, Lansing, MI, Jun. 2021, paper THPTEV016, unpublished.

[4] H. Hu, D. Bafia, and Y.-K. Kim, “Evaluating the Effects of Nitrogen Doping and Oxygen Doping on SRF Cavity Performance”, in *Proc. IPAC’22*, Bangkok, Thailand, Jun. 2022. doi: 10.18429/JACoW-IPAC2022-TUPOTK034

[5] D. Bafia, A. Grassellino, and A. Romanenko, “The Anomalous Resonant Frequency Variation of Microwave Superconducting Niobium Cavities Near  $T_c$ ”, arXiv, 2021. doi: 10.48550/arXiv.2103.10601

[6] D. Bafia, “Exploring and Understanding the Limitations of Nb SRF Cavity Performance”, Ph.D. thesis, Phys. Dept., Illinois Institute of Technology, Chicago, IL, 2020.

[7] M. Martinello *et al.*, “Effect of interstitial impurities on the field dependent microwave surface resistance of niobium”, *Appl. Phys. Lett.*, vol. 109, pp. 062601, 2016. doi: 10.1063/1.4960801

[8] J.C. Slater, “Microwave Electronics”, *Rev. Mod. Phys.*, vol. 18, pp. 04441, 1946. doi: 10.1103/RevModPhys.18.441

[9] J. Halbritter, “Fortran-program for the computation of the surface impedance of superconductors,” in *KFK-Extern*, vol. 3/70-6, 1970. doi: 10.5445/IR/270004230.

[10] G. Ciovati, “Effect of low-temperature baking on the radio-frequency properties of niobium superconducting cavities for particle accelerators”, *J. Appl. Phys.*, vol. 96, pp. 1591–1600, 2004. doi: 10.1063/1.1767295

[11] A. Romanenko *et al.*, “First Direct Imaging and Profiling TOF-SIMS Studies on Cutouts from Cavities Prepared by State-of-the-Art Treatments”, in *Proc. SRF’19*, Dresden, Germany, Jul. 2019. doi: 10.18429/JACoW-SRF2019-THP014

[12] A. Romanenko *et al.*, “Effect of mild baking on superconducting niobium cavities investigated by sequential nanoremoval”, *Phys. Rev. ST Accel. Beams*, vol. 16, pp. 012001, 2013. doi: 10.1103/PhysRevSTAB.16.012001